frontiers

Supplementary Material

GRID CHARACTERIZATION

Temporal resolution differences

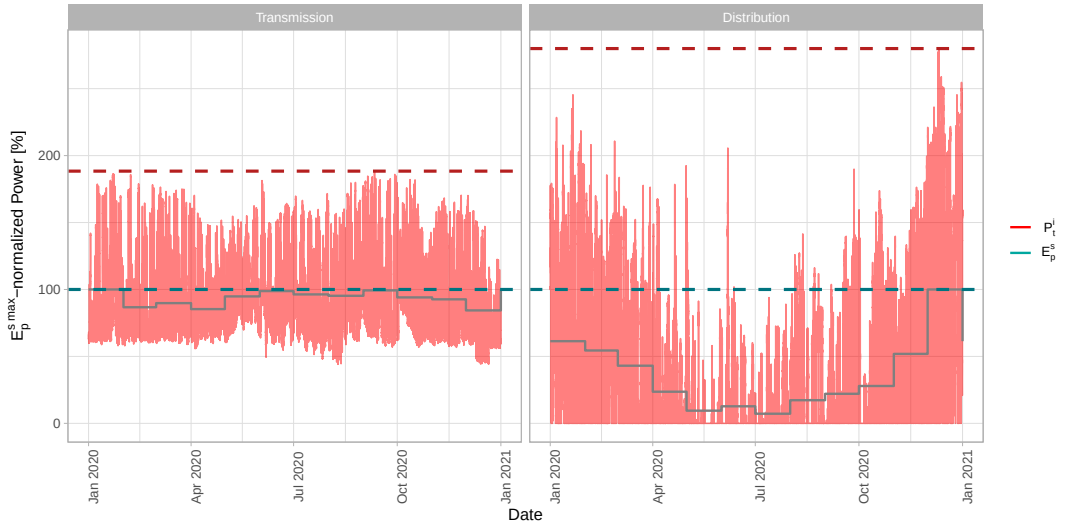

Figure S1. Time evolution of the observed $\mathbf{P_g}$ $[\mathrm{GW}^{15\mathrm{min}}]$ and the modeled power curves $\dot{\mathbf{E}}_{\mathbf{g}}^{\mathbf{s}}$ $[\mathrm{GW}^{\mathrm{TP}}]$ for transmission and distribution, normalized by the maximum modeled power $\dot{E}_g^{s,max}$ $[\mathrm{GW}^{\mathrm{TP}}]$ (Swissgrid, 2022). The ratio between the maximum of the power curves (dashed) corresponds to the observation coefficient $\boldsymbol{k_g^{\dot{E}\leftrightarrow P}}$.

In order to assess differences between real world installations and the computer model, we integrate $k_g^{i\leftrightarrow j}$ scaling factors. We distinguish three different powers

1. $\dot{E}_g^s$ the power modeled in EnergyScope with an average power over the typical modeling period TP $\left[\mathrm{GW}^{TP}\right]$
2. P_g^i the power measured in the network at a frequency of 15 minutes $\left[\mathrm{GW}^{15\mathrm{min}}\right]$
3. S_g^{inst} the installed network power estimated by an engineer, to satisfy the instantaneous power variations $[\mathrm{GW}^{\mathrm{instantaneous}}]$

Figure S1 depicts the he estimation of the safety coefficient between observation (1) and installation (2), which is performed by calculating the ratio of the maxima of the averages between the measured data P_g^i $\left[\mathrm{GW}^{15\mathrm{min}}\right]$ to the sizes of the installed transformers (Gupta et al., 2021). We therefore proceed at identifying the maximum annual power per transformer of voltage level $P_g^{i,max}$ at the typical installation size of the transformer S_g^{inst}, from which the installation safety coefficient $k_g^{P\leftrightarrow S}$ can be estimated.

Grid parameters

The grid parameters are summarised in table S1 while the technical details and sources of the different parameters can be accessed in `https://gitlab.com/ipese/on-the-role-of-energy-infrastructure-in-the-energy-transition`. The confidence interval has been selected as $\pm 25\%$, except for the reference length l_g^{ref}, where the validation showed a cumulative error of $\pm 23.1\%$, as for the scaling factors varying $\boldsymbol{k_g^{P \leftrightarrow S}} = 3^{+0.18}_{-0.40}$ and $\boldsymbol{k_g^{\dot{E} \leftrightarrow P}} = 2^{+0.76}_{-0.11}$.
The approach to assess the those differences can be applied to a different time resolution, such as the for example the hourly one (Limpens et al., 2019). In latter case, we are be able to better assess the load variations throughout the year and therefore leads to a higher $\boldsymbol{k_g^{\dot{E}[h] \leftrightarrow S}} = 2.93^{+1.13}_{-0.15}$.

Table S1. Grid infrastructure techno-economic characterization with uncertainty bounds of electricity grid, methane and hydrogen pressure grid, split in the four power levels. Case study for a geographically averaged Swiss energy system, based on the deployed capacities in 2020.

	Confidence	EHV/P			HV/P			MV/P			LV/P		
	Interval	Elec.	CH_4	H_2[1]	Elec.	CH_4	H_2[1]	Elec.	CH_4	H_2[1]	Elec.	CH_4	H_2[1]
l_g^{tot} [10^3km]	$\pm 25\%$	6.7	0.71	0.71	8.9	0.94	0.94	43	4.35	4.35	130	9.7	9.7
n_g [$-$]	$\pm 25\%$	137	20	20	775	116	116	15490	2039	2039	2.2 M	440 k	440k
l_g^{ref} [km]	$\pm 23.1\%$[2]	48.9	35.5	35.5	11.5	8.10	8.10	2.8	2.13	2.13	0.06	0.11	0.11
S_g^{θ} [MW]	$\pm 25\%$	1700	51500	12133	500	6140	1557	30	425	132	0.3	0.425	0.2
C_g^{inv} [MCHF/kmGW]	$\pm 25\%$	3.4	0.0768	0.326	5.2	0.227	0.895	53.3	0.484	1.557	500	13.593	55.7

[1] Hydrogen grid infrastructure not existing yet. For modeling and comparison purposes, assumed to be equal to the natural gas pressure grid.
[2] Precision according to the cumulative error of the grid length equidistant estimation to the reported length by Gupta et al. (2021).

Grid infrastructure

Applying a geographical averaged model, leads to uncertainty related to the characterization of the existing infrastructure. We assess latter uncertainty by analyzing the reported electric transformer sizes at different levels from Gupta et al. (2021). The confidence interval of the distribution is reported in table S2. We observe that with decreasing voltage level, the $95\,\%$ confidence interval is increasing from $27.6\,\%$ up to $72.4\,\%$. The applied methodology is therefore subject to the limitation of the uncertainty in the distribution level. In order to resolve this limitation and assess the role of self-sufficiency and decentralization, we need to integrate the role of districts within the global energy system, publication currently in redaction.

Table S2. Grid size validation by assessing the reported value with the geographic distribution reported by Gupta et al. (2021).

Level	S_g^{θ} [MW]	S_g^{min} [MW]	S_g^{max} [MW]	$S_g^{95\%}$ [MW]
EHV	1700	1246.67	2153.33	$1721.4^{+431.2}_{-474.7}$
HV	500	193.55	806.45	$470.6^{+152.9}_{-138.3}$
MV	30	1.62	58.38	$32.5^{+0.962}_{-17.5}$
LV	0.3	0.05	0.55	$0.29^{+0.15}_{-0.21}$

VALIDATION

Table S3. Validation of the EnergyScope model by simulating the 2020 energy system configuration by primary energy consumption [TWh]. Comparison of actors.

Resource	**BFE**	**Energy System simulation**		**Economic optimization**	
		EnergyScope	Difference	EnergyScope	Difference
Coal	1.01	0.88	-0.13	0	-1.01
Gasoline	23.91	23.44	-0.47	0	-23.91
Diesel	30.55	31.65	1.1	0	-30.55
CH_4	31.35	31.69	0.34	0	-31.35
LFO	27.05	26.58	-0.47	0	-27.05
Nuclear	44.6	43.78	-0.82	0	-44.6
Solar PV	2.6	2.62	0.02	52.31	49.71
Water	40.61	40.61	0	40.61	0
Wind	0.15	0.14	-0.01	21.02	20.87
Waste	16.79	17.04	-0.25	19.75	-2.96
Wood	10.97	11.16	0.19	15.28	4.31
Total	**229.59**	**229.59**	**0**	**148.97**	**-80.62**

The simulation of energy system configurations is subject to the assumption of minimizing total system costs and to climate target constraints, corresponding to a economically reasonable thinking being. When simulating the 2020 energy system, we notice a difference between the minimum cost system, proposed as a solution by the model, and the real system, installed in 2020. This difference can be explained by the assumed perspectives of the different actors that can be simulated by the model. History did not choose to install the most economical solution for the whole, but tries to optimize his personal well-being with a certain inertia, resulting from a multitude of sometimes contradictory information sources. At the implementation level, the tendency to conserve the existing system means adding constraints to the economic optimization model in order to reproduce the 2020 configuration.

In order to validate the model, both behavioral perspectives were applied and summarized in table S3. The additional constraint applied to historical configuration is to reproduce, by minimizing the total difference, the primary energy consumption reported in the Swiss Global Energy Statistics (Kost, Michael, 2021). Then, the results obtained for the two configurations are compared to the real Swiss system.

The major differences between the optimization and simulation resuts in 2020 can be explained by (i) more efficient conversion technologies in the EnergyScope model than those installed in 2020 and (ii) the use of resources for purposes other than those modeled. Due to the constraint imposed, the model exactly reproduces the total primary consumption. However, the largest differences are observed in the share of fossil and nuclear energy used.

The solutions reported for the optimization illustrate the difference in total configuration. The economic optimization under the constraints of climate neutrality (no net CO2 emissions) and independence (without imports) leads the model to a fully renewable and more efficient energy system, with primary energy consumption reduced by $80.62\,\mathrm{TWh}$, or -29%, compared to the total primary energy consumption of $278\,\mathrm{TWh}$.

GRID REINFORCEMENT IN ECONOMIC OPTIMIZATION

Uncertainty analysis

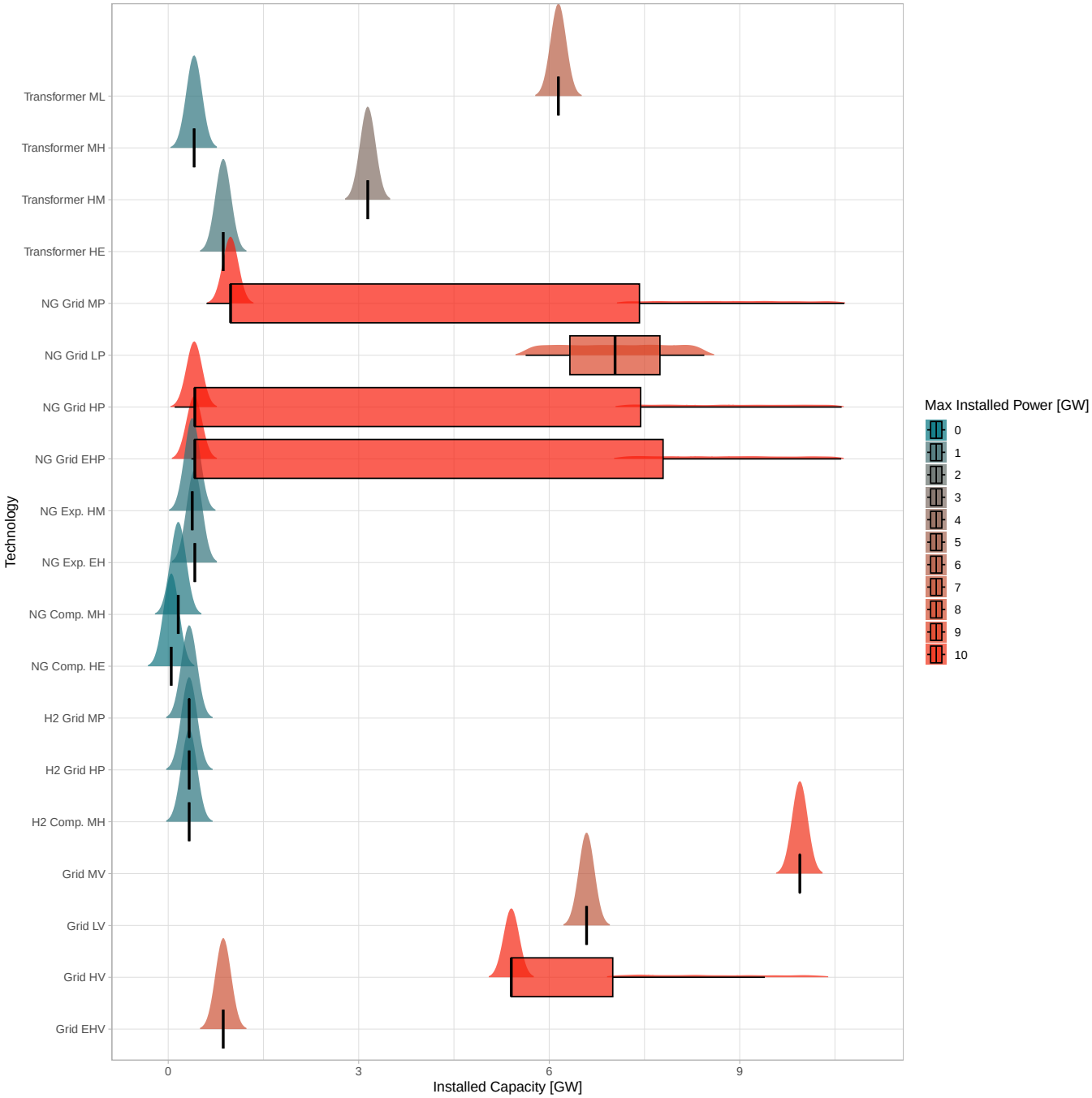

Figure S2. Frequency of appearance and Boxplot of the installed distribution technologies size applying the Monte-Carlo approach.
Case study of the economic optimization of a neutral (no net emissions) and independent (no imports) Swiss energy system in 2050.

The uncertainty analysis applied to the energy-independence and CO_2-neutrality case study of Switzerland led to different energy system configurations characterized by different installed capacities. Figure S2

Table S4. Grid installed capacities peaks, for the Swiss 2050 neutral and independent energy system configuration economic optimization under 50 000 Monte Carlo iterations.
The value in brackets correspond to the probability of the peak, according to the frequency of appearance within the uncertainty analysis.

Grid	Power level	Existing capacity $\mathbf{S_g^{inst,ext}}$ [GW]	Peak 1 $\mathbf{S_g^1}$ [GW]	Peak 2 $\mathbf{S_g^2}$ [GW]
Elec.	EHV	$6.297^{+0.787}_{-0.787}$	$1.064^{+0.013}_{-0.695}$ (100 %)	-
	HV	$8.668^{+1.086}_{-1.086}$	$5.434^{+0.093}_{-0.028}$ (93.9 %)	$7.843^{+1.623}_{-1.459}$ (6.1 %)
	MV	$5.574^{+0.697}_{-0.697}$	$10.185^{+0.047}_{-0.089}$ (100 %)	-
	LV	$4.150^{+0.519}_{-0.519}$	$6.589^{+0.000}_{-0.000}$ (100 %)	-
Methane	EHP	$8.838^{+1.101}_{-1.1012}$	$0.445^{+0.044}_{-0.122}$ (94.6 %)	$8.838^{+1.009}_{-1.018}$ (5.4 %)
	HP	$8.838^{+1.101}_{-1.01}$	$0.472^{+0.036}_{-0.074}$ (94.6 %)	$8.838^{+1.017}_{-1.008}$ (5.4 %)
	MP	$8.876^{+1.110}_{-1.110}$	$0.903^{+0.029}_{-0.264}$ (94.5 %)	$8.876^{+1.081}_{-1.077}$ (5.5 %)
	LP	$7.036^{+0.880}_{-0.880}$	$6.395^{+1.018}_{-1.001}$ (100 %)	
Hydrogen	EHP	-	-	-
	HP	-	$0.330^{+0.000}_{-0.037}$ (100 %)	-
	MP	-	$0.330^{+0.003}_{-0.037}$ (100 %)	-
	LP	-	-	-

depicts the frequency of appearance and distribution technologies at a given installed capacity. It is possible to distinguish between three types of distributions; (i) the robust solutions, where independent of the variation, the capacity remains constant, such as EHV Grid or the NG transformers, (ii) almost uniform spread out technologies (NG Grid LP) and (iii) technologies with multiples peaks (Grid EHV, NG Grid EHP).
It is the third category indicating the reaching of a tilting point towards the switching of another configuration rather than continuously moving. Identifying correlations between peaks of different configurations under uncertainty is a point to be treated in a future publication.
The robustness of the model can be assessed by assessing the peak distribution and attributing the probability of appearance (figure S2). The results are summarized in table S4 and show, that the deployed capacity of the grids is robust at a minimum level of $94.5\,\%$. It can be noted, that the apparition of secondary peaks is due to the uncertainty relying on the estimation of the existing capacity of the grids, as the secondary peaks in the methane grids are following the uncertainty distribution of the existing capacity $\pm 25\%$.

Seasonal intermittence

Besides the installed power, the configuration is subject to the seasonal operation of the capacities. Figure S3 depicts the monthly average use of the technologies corresponding to the median configuration of the case study.
It is possible to identify three types of technologies; (i) constant technologies, responding to annually constant demands such as industry or freight mobility, (ii) seasonal intermittent technologies such as the renewable energy carriers or technologies responding to seasonal varying demands such as domestic heating, and (iii) the back-up technologies to compensate for the reaching of a potential limitation or seasonal discrepancy.
We can observe that distribution technologies are following the same pattern, where (i) the hydrogen technologies are used at constant rate to power the freight hydrogen technologies, (ii) the distribution grid

follows the intermittency of the wind and photovolotaics variations, and (iii) the methane gas expanders are correlated to the natural gas storage emptying.

Figure S3. Seasonal utilization of the technologies.
Case study of the economic optimization of a neutral (no net emissions) and independent (no imports) Swiss energy system in 2050.

THE ROLE OF GRID REINFORCEMENT

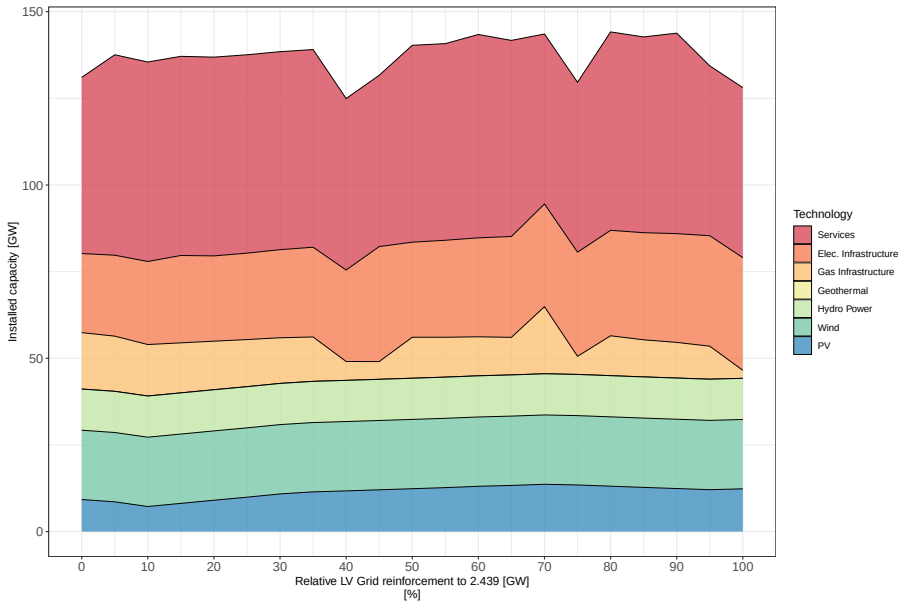

Figure S4. Evolution of the installed capacities of the Swiss energy system according to LV grid reinforcement according to the energy system costs in Figure 9 (a) of the main paper.
Case study of the economic optimization of a neutral (no net emissions) and independent (no imports) Swiss energy system in 2050.

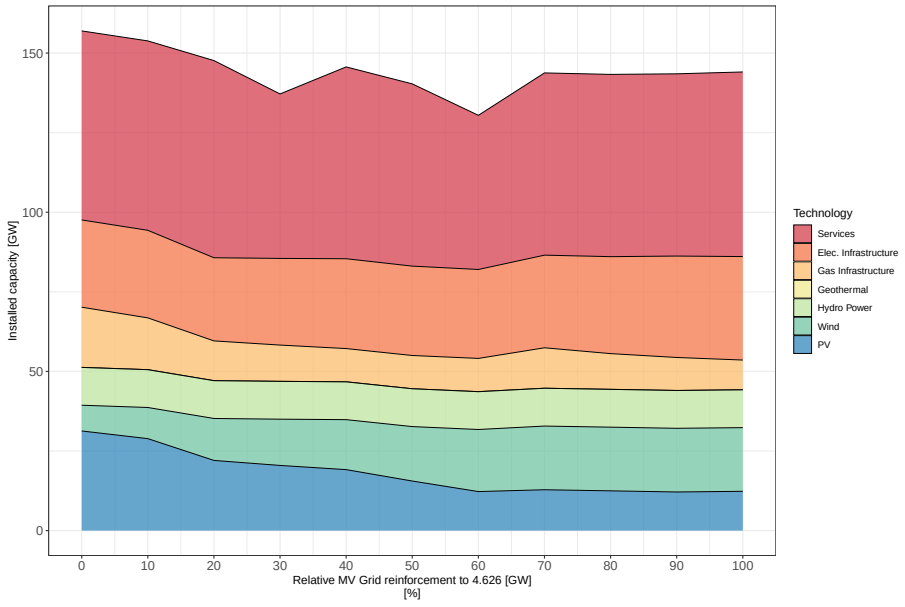

Figure S5. Evolution of the installed capacities of the Swiss energy system according to MV grid reinforcement according to the energy system costs in Figure 9 (b) of the main paper.
Case study of the economic optimization of a neutral (no net emissions) and independent (no imports) Swiss energy system in 2050.

THE INTERPLAY OF WIND AND PHOTOVOLTAICS

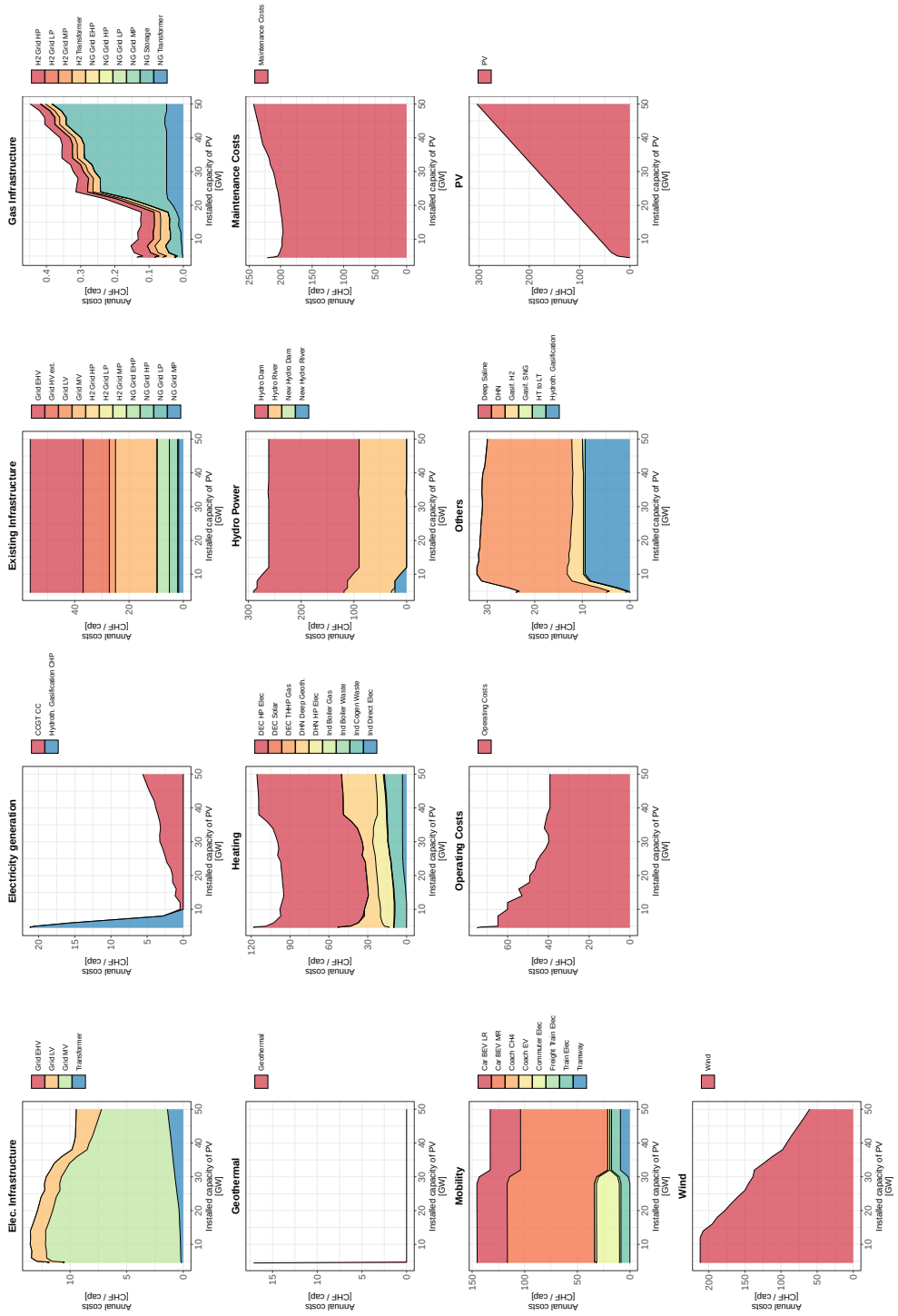

Figure S6. Evolution of detailed investments of the Swiss energy system according to PV penetration in 2050.
Case study of the economic optimization of a neutral (no net emissions) and independent (no imports) Swiss energy system in 2050.

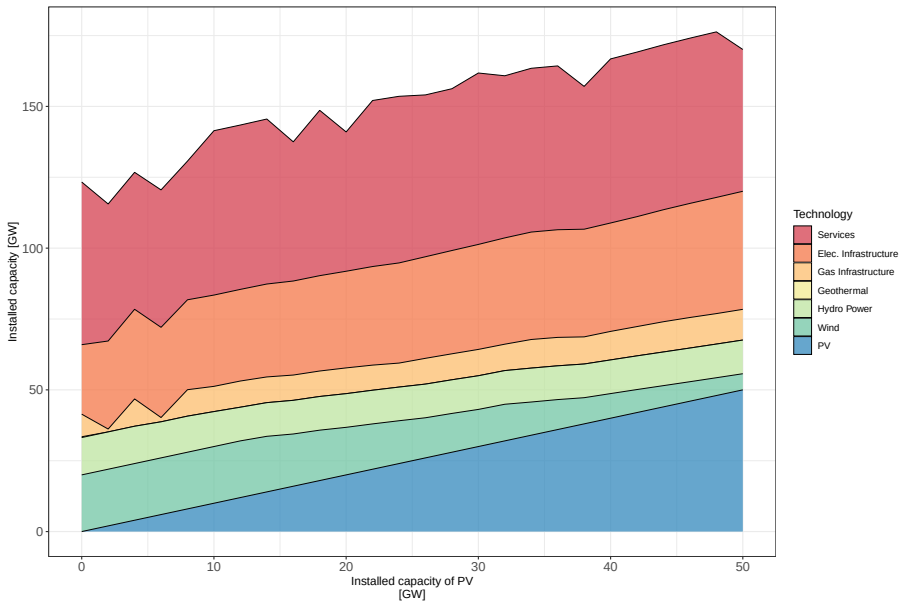

Figure S7. Evolution of installed capacities of the Swiss energy system according to PV penetration in 2050 according to the energy system costs in Figure 11 of the main paper.
Case study of the economic optimization of a neutral (no net emissions) and independent (no imports) Swiss energy system in 2050.

ABOUT THE NON-CONTINUOUS EVOLUTION OF THE DEPLOYED CAPACITIES

Figures S4, S5 and S7 represent the installed power of the different technologies from figures 9 and 11 in the main paper. One can observe the jumps in the total power deployed along the parametrization, which results in a gradual evolution within the total cost composition. One can therefore expect to have the same smooth behavior in the total capacities deployment as in the total cost evolution.

These jumps indicate switches in the energy system configuration, whose origin can be located in the mixed integer linear type of the model, generating equivalent solutions from the objective function point of view. In order to prove the latter hypothesis, the configuration at $20\,\mathrm{GW}$ of photovoltaic deployment, as observed in figure S7 has been interpolated with the capacities at the upper ($22\,\mathrm{GW}$) and lower ($18\,\mathrm{GW}$) configurations, and entered as constraints in the model. The resulting cost differs by 8.07×10^{-11} from the original cost, value being under the *mipgap* threshold of 1×10^{-10} and therefore equivalent from the optimisation point of view.

The existence of equivalent solutions from an economic optimization point of view is not expected to affect the presented results, as the uncertainty analysis depicted the validity range of the methodology presented. However, exploring and identifying the space of equivalent solutions from an economic optimization point of view within a MILP problem will be subject to a future publication.

REFERENCES

Gupta, R., Sossan, F., and Paolone, M. (2021). Countrywide PV hosting capacity and energy storage requirements for distribution networks: The case of Switzerland. *Applied Energy* 281, 116010. doi:10/gmnvcm

Kost, Michael (2021). *Gesamtenergiestatistik 2020*. Tech. Rep. 10537, BFE, Bern

Limpens, G., Moret, S., Jeanmart, H., and Maréchal, F. (2019). EnergyScope TD: A novel open-source model for regional energy systems. *Applied Energy* 255, 113729. doi:10.1016/j.apenergy.2019.113729

[Dataset] Swissgrid (2022). Aggregated energy data of the control block Switzerland